Fuzzy-sliding mode control of a full car semi-active suspension systems with MR dampers

L. Zheng and Y. N. Li

State Key Laboratory of Mechanical Transmission, Chongqing University, Chongqing 400044, P.R. China

A. Baz*

Department of Mechanical Engineering, University of Maryland, College Park, MD 20742, USA

(Received October 16, 2006, Accepted October 12, 2008)

Abstract. A fuzzy-sliding mode controller is presented to control the dynamics of semi-active suspension systems of vehicles using magneto-rheological (MR) fluid dampers. A full car model is used to design and evaluate the performance of the proposed semi-active controlled suspension system. Four mixed mode MR dampers are designed, manufactured, and integrated with four independent sliding mode controllers. The siding mode controller is designed to decrease the energy consumption and maintain robustness. In order to overcome the chattering of the sliding mode controllers, a fuzzy logic control strategy is merged into the sliding mode controller. The proposed fuzzy-sliding mode controller is designed and fabricated. The performance of the semi-active suspensions is evaluated in both the time and frequency domains. The obtained results demonstrate that the proposed fuzzy-sliding mode controller can effectively suppress the vibration of vehicles and improve their ride comfort and handling stability. Furthermore, it is shown that the "chattering" of the sliding mode controller is smoothed when it is integrated with a fuzzy logic control strategy. Although the cost function of the fuzzy-sliding mode control is a slightly higher than that of a classical LQR controller, the control effectiveness and robustness are enhanced considerably.

Keywords: MR fluid damper; semi-active suspension; fuzzy-sliding mode controller.

1. Introduction

Recently, suppression of the vibration of vehicles has been a very active research area which aims primarily at attenuating the disturbances resulting from various road excitations. This is normally accomplished by employing a wide variety of vehicle suspension systems. The conventional passive suspension systems featuring oil damper provide design simplicity and cost-effectiveness. However, the performance improvements are effective only over a narrow frequency range. Active suspension systems provide high control flexibility over a wider frequency range. Nonetheless, high energy requirements, complicated control systems including sensors, actuators and control logic limit their wider acceptance. The semi-active suspension systems, which consist of passive springs and controllable dampers, are recognized to be a better practical solution for enhancing the performance of suspension systems and improving the ride comfort. Most of these systems rely in their operation on Magneto Rheological (MR) dampers because of their potential use as semi-active control devices (Sean 2001, Yao, *et al.* 2002). The feasibility of these devices has been successfully demonstrated in numerous civil engineering applications (Yang, *et al.* 2002, Dyke, *et al.* 1996). Several MR dampers were developed in University of Nevada, including the MR dampers for mountain bicycle (Breese and Gordaninejad 2003), motorcycle (Ericksen and Gordaninejad 2000), High Mobility Multi-Purpose Wheeled Vehicle (HMMWV) (Gordaninejad and Kelso 2000), and high-payload, off-highway vehicle (Gordaninejad and Kelso 2000). The first industrial semi-active suspension system using MR dampers in vehicles has been demonstrated in Delphi Corporation.

However, integration of the MR dampers into suspension systems poses serious challenges as the MR dampers are highly nonlinear and the parameters that govern the vehicle dynamics are often uncertain due to changes in the loading conditions such as the number of passengers and payload. Such challenges can be overcome by using robust control algorithms. Song and Ahmdian (2004) studied two semi-active adaptive control algorithms for a heavy-duty truck seat suspension with MR damper. These algorithms include: the non-model based skyhook control and model-based nonlinear adaptive control algorithms. The study showed that the model-based adaptive control provides a robust performance. The main disadvantage of the model-based adaptive control approach is the large amount of flops, which significantly increases the system implementation cost. Man, *et al.* (2005) used a simple sky-hook controller of a semi-active suspension for a fork lift truck with MR dampers. The field tests have demonstrated a substantial comfort improvement with respect to the passive suspension. Liu, *et al.* (2003) presented a theoretical study to examine the behavior a fail-safe MR damper based on a temperature compensated sky-hook strategy for a quarter car model of a High Mobility Multipurpose Wheeled Vehicle (HMMWV). The obtained results demonstrated that the compensated sky-hook control system can reduce the sprung mass displacement and acceleration compared to the uncompensated sky-hook control system. Thus, a good ride comfort is obtained. Wang, *et al.* (2003) proposed a semi-active force tracking PI controller for a quarter-vehicle model with MR damper. The vibration attenuation performance of the MR damper using the semi-active force tracking proportional-integral (PI) control algorithm is analyzed and evaluated. The obtained results showed that the proposed control algorithm can yield superior vibration attenuation of the sprung mass resonance and in the vicinity of the wheel-hop. Choi, *et al.* (2002) studied the control characteristics of a full-car suspension featuring a semi-active MR fluid damper. The governing equations of motions were derived and incorporated with sky-hook controller. Control characteristics of the full-car suspension installed with the MR damper were evaluated through hardware-in-the-loop simulation (HILS). Bump and random tests showed that both ride quality and steering stability could be substantially improved. Choi, *et al.* (2003) used a sliding mode controller (SMC) to attenuate the vibration of a semi-active seat suspension with an ElectroRheological (ER) fluid damper. A hardware-in-the-loop simulation (HILS) is undertaken to demonstrate a practical feasibility. An improvement in ride comfort quality under various road conditions is demonstrated. Choi, *et al.* (2000) extended his work to a full-car suspension system featuring ER dampers and found it to equally effective. Liu, *et al.* (2001) presented a closed-loop control system based on fuzzy logic to suppress the bridge deck motion via MR dampers under random excitations. The experimental results showed that fuzzy control system can significantly reduce the relative deck displacement. Yokoyama, *et al.* (2001) proposed a model following sliding mode controller for semi-active suspension systems with MR damper. Numerical simulations illustrated a high robustness of the sliding mode controller against model uncertainties and disturbance. Other control algorithms are also used to control the vibration of civil structures with MR dampers such as Lyapunov control (Leitmann 1994), decentralized bang-bang control (McClamroch and Gavin 1995), modulated homogeneous friction (Inaudi 1997), bi-state control (Patten, *et al.* 1994a), fuzzy logic control (Sun and Goto 1994), and clipped-optimal (Patten, *et al.* 1994b).

Sliding mode control has been widely accepted as a robust control algorithm for many years. Nowadays, sliding mode controllers (SMCs) have been widely applied in numerous areas, such as in general motion control, robotics, process control and aerospace and vehicle applications. The main reason for this popularity is their attractive advantages such as good control performance of nonlinear systems with uncertainties in the presence of disturbances, stable control, robustness, and applicability to multiple-input-multiple-output (MIMO) systems. The most significant property of SMCs is their robustness. Simple speaking, this means that when a system is in a sliding mode, it is insensitive to parameter changes or to external disturbances. The main drawback of the SMC is "chattering" which can excite undesirable high-frequency dynamics. Several methods of chattering reduction have been reported. One approach (Slotine and Sastry 1983) places a boundary layer around the switching surface such that the relay control is replaced by a saturation function. Another method (Lord 1999) replaces a max–min-type control by a unit vector function. However, these approaches provide no guarantee of convergence to the sliding mode and involve a tradeoff between chattering and robustness.

Fuzzy logic control (FLC) has been considered as one of the most efficient methods in addressing the inherent control problems related to nonlinear systems that contain uncertainties. In this paper, the smooth control feature of the FLC is used to overcome the "chattering" of the SMC for a full car semi-active suspension with MR dampers. A novel fuzzy-sliding mode controller is designed and formulated. The control characteristics of a full-car suspension system featuring MR dampers for a passenger vehicle integrated with a FSMC (fuzzy-sliding mode control) controller is evaluated in both the time and frequency domains by considering bump and random excitation conditions.

2. MR damper

In this study, mixed mode MR dampers are designed and manufactured. The schematic drawing of the MR damper is shown in Fig. 1. This is a classic twin tube MR damper with two coils which is integrated in the front suspension of a mini-bus (model: SC6350, produced in China). It has two fluid reservoirs, one inside the other. This inner housing is filled with MR fluid so that no air pockets exist. To accommodate the volumetric changes due to piston rod movement, the outer housing that is partially filled with MR fluid is used. In practice, a valve assembly called a "foot valve" is attached to the bottom of the inner housing to regulate the flow of fluid between the two reservoirs. As the piston rod enters the damper, MR fluid flows from the inner housing into the outer housing through the foot valve. The amount of fluid flowing from the inner to the outer housing is equal to the volume displaced by the piston rod. As the piston rod retracts the MR fluid starts flowing into the inner housing through the return valve. When the piston moves in the inner housing, the MR fluid flows through the duct between the piston and the inner housing. If an electric current is passed into coils, an additional damping force is generated by the yield stress of the MR fluid.

The design challenge is to develop a DC electromagnetic circuit that can generate sufficient flux across the MR-gap in a minimum amount of time. Innovative drilling techniques were developed to drill very long holes, with $L/D > 60$, to pass the wires that feed the electromagnetic coils as shown in Fig. 1. The coils generate the magnetic field necessary to activate the MR fluid. Adjacent spools are

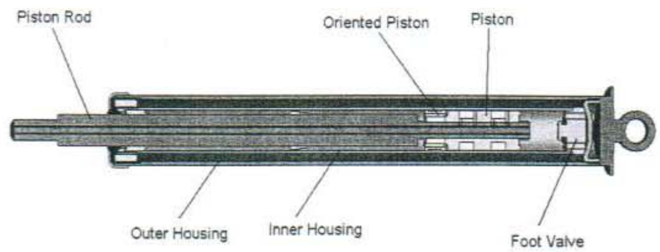

Fig. 1 The schematic diagram of the MR damper

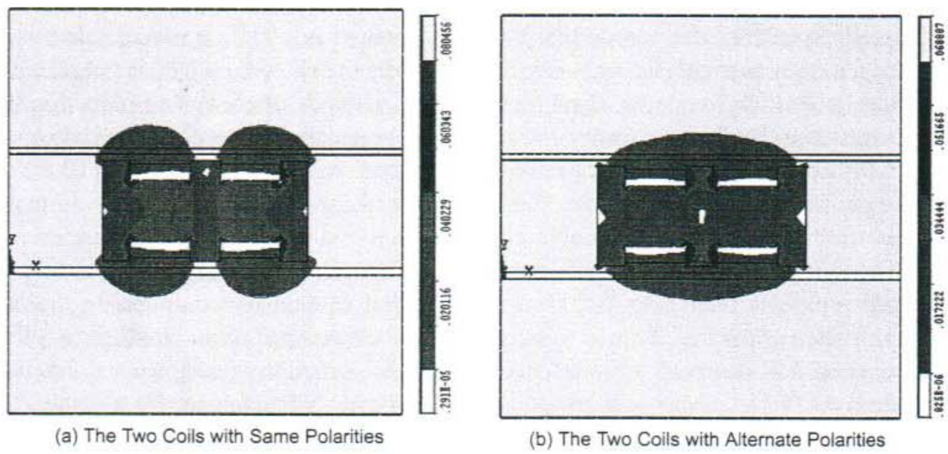

Fig. 2 Magnetic flux density with different winding orientations

wound in opposing directions and the magnetic flux forms three magnetic circuits. The benefit of using two different coils, instead of one single long coil, is that the overall inductance of the circuit is much lower and consequently the time response is shorter (Sean 2001).The goal of alternating the polarities is to strengthen the magnetic field taking place between two adjacent cores. The results of a finite element analysis show the different between the same polarity (or winding orientation) and the alternate polarity arrangements as displayed in Fig. 2. The available copper wire diameter is 0.5mm, available internal space allows 450 turns for each spool.

For standard applications, the current density of copper wire may be varying from 4 to 8 amperes per square mm, depending on the type of isolation, the type of environment and the type of cooling devices. In the present MR damper, the maximum current is limited to 1.5 amperes resulting in a maximum current density of 7.64 amperes per square mm.

The MR damper contains 300 ml MR fluid supplied by Chongqing Instrument Material Research Institute. Fig. 3 shows the prototype MR damper and its associated components. Using the experimental set-up shown in Fig. 4, the behavior of the MR damper can be characterized. Experiments were conducted at a peak-to-peak amplitude of 25 mm, frequency of 0.64, 1.28, 1.92 Hz and current of 0, 0.5, 1.0A.

As shown in Fig. 1, when the piston rod enters the damper, the MR fluid is forced to flow through MR channel under pressure, on the other hand, the MR fluid is sheared due the movement of the piston. This means the MR fluid works in a mixed mode which is a combination of pressure driven mode and shear mode. For mixed operational mode, the damping force can be derived by regarding the mixed

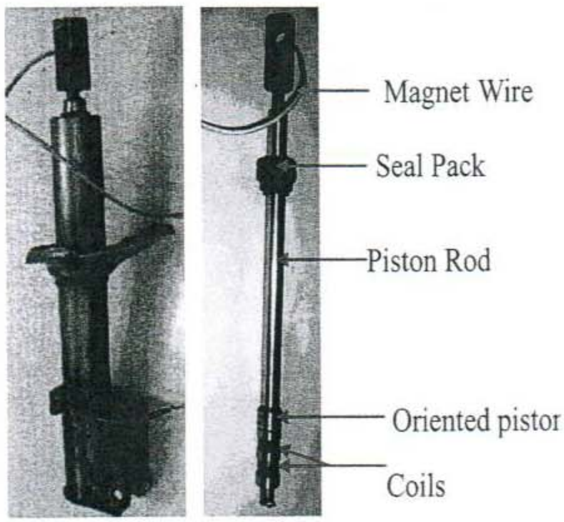

Fig. 3 The prototype MR damper

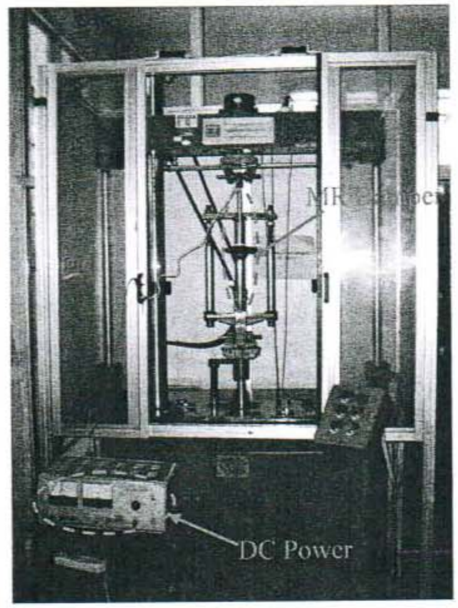

Fig. 4 The experimental set-up

mode as the combination of flow mode and shear mode:

$$F_{DAMPER} = \left[\frac{18\eta l A_p^2}{\pi R_1(R_2-R_1)^3} + \frac{6\pi R_1 l\eta}{R_2-R_1}\right]\dot{x}_p + \left[\frac{9lA_p}{R_2-R_1} + 6\pi R_1 l\right]\tau_y \tag{1}$$

where A_p is the working area of the piston, η is viscosity of the MR fluid without the magnetic field applied, l is the length of each duct, R_2 is inner radius of the inner housing, R_1 is the outer radius of the piston. In additional, the duct is divided into three parts by two coils, we assume that each part has the same length.

In order to express the damping force in a simple way and apply it to the full car model, Eq. (1) can be rewritten as follows:

$$F_{DAMPER} = C_s\dot{x}_p + F_{MR}sign(\dot{x}_p) \tag{2}$$

where, $C_s = \dfrac{18\eta l A_p^2}{\pi R_1(R_2-R_1)^3} + \dfrac{6\pi R_1 l\eta}{R_2-R_1}$, and $F_{MR} = \left[\dfrac{9lA_p}{R_2-R_1} + 6\pi R_1 l\right]KH^{\beta}$

Here, C_s is the equivalent viscous damping coefficient of the MR damper. F_{MR} is the controllable damping force of the MR damper. K and β are the characteristic constants of the MR fluid used in the MR damper. For the MR fluid used in the MR damper, $K = 0.0618$ and $\beta = 1.25$. The parameters for MR damper are listed in Table 1.

Fig. 5 shows a comparison between the theoretical and experimental force-displacement characteristics of the MR damper at different control currents. The displayed characteristics are obtained for a sinusoidal excitation frequency of 1.96 Hz with an excitation amplitude of 25 mm. It

Table 1 Material and geometric parameters of the MR damper

η	5 Pa.s	R_2	1.55×10^{-4} m
K	0.0618	R_1	1.40×10^{-4} m
β	1.25	N	450
l	7×10^{-3} m	D_p	2.8×10^{-4} m
A_p	6.1575×10^{-4} m^2		

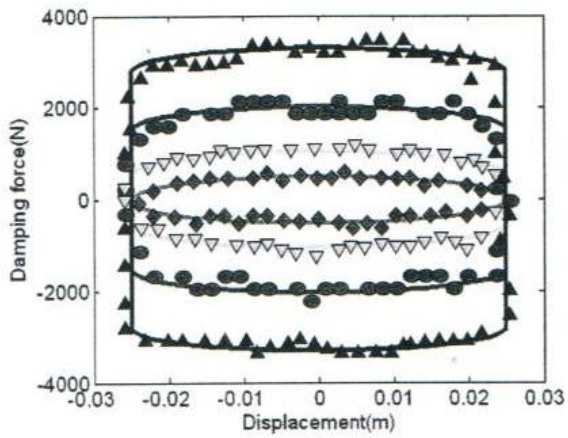

Fig. 5 Force-displacement loop for MR damper (input current = 0, 0.4, 0.8, 1.2A)
1.2A —Theoretical ▲ Experimental, 0.8A —Theoretical ●Experimental
0.4A —Theoretical ▼Experimental, 0A —Theoretical ◆Experimental

can be seen that the theoretical predictions are in close agreement with the experimental results. Hence, Eq. (2) can be accurately used to design the full-car semi-active suspension system with MR dampers.

3. The dynamics and sliding mode controller

3.1. Dynamic model

A dynamic model for a full-car semi-active suspension system via MR dampers is constructed in Fig. 6. The governing equations of motion can be derived as follows:

$$M\ddot{h}+f_{ks1}+f_{ks2}+f_{ks3}+f_{ks4}+f_{cs1}+f_{cs2}+f_{cs3}+f_{cs4} = F_{MR1}+F_{MR2}+F_{MR3}+F_{MR4},$$

$$I_{xx}\ddot{r}+(f_{ks1}+f_{cs1})l_{ylf}-(f_{ks2}+f_{cs2})l_{ylf}+(f_{ks3}+f_{cs3})l_{lyr}-(f_{ks4}+f_{cs4})l_{ylr} = F_{MR1}l_{ylf} \quad ,$$
$$-F_{MR2}l_{ylf}+F_{MR3}l_{ylr}-F_{MR4}l_{ylr}$$

$$I_{yy}\ddot{p}-(f_{ks1}+f_{cs1})l_{xf}-(f_{ks2}+f_{cs2})l_{xf}+(f_{ks3}+f_{cs3})l_{xr}+(f_{ks4}+f_{cs4})l_{xr} = -F_{MR1}l_{xf},$$
$$-F_{MR2}l_{xf}+F_{MR3}l_{xr}+F_{MR4}l_{xr}$$

$$M_{w1}\ddot{z}_{w1}-f_{ks1}-f_{cs1}+f_{kt1} = -F_{MR1},$$

$$M_{w2}\ddot{z}_{w2} - f_{ks2} - f_{cs2} + f_{kt2} = -F_{MR2},$$

$$M_{w3}\ddot{z}_{w3} - f_{ks3} - f_{cs3} + f_{kt3} = -F_{MR3},$$

and

$$M_{w4}\ddot{z}_{w4} - f_{ks4} - f_{cs4} + f_{kt4} = -F_{MR4}.$$

where $f_{ksi} = k_{si}(z_{bi} - z_{wi})$, $f_{csi} = c_{si}(\dot{z}_{bi} - \dot{z}_{wi})$, $f_{kti} = k_{ti}(z_{wi} - w_i)$ for $i = 1,2,3,4$. M is the sprung mass and M_{wi} ($i = 1,2,3,4$) is the unsprung mass. I_{xx} and I_{yy} are the roll and pitch mass moment of inertia. k_{si} ($i = 1,2,3,4$) is the stiffness coefficient of the suspension. c_{si} ($i = 1,2,3,4$) is the damping coefficient of the suspension, and it is equal to C_s in Eq. (2). k_{ti} is the stiffness coefficient of the tire. h, r and p are the vertical displacement, roll and pitch angular displacement. l_{xf} and l_{xr} are the distance between the front suspension and center of gravity of sprung mass (C.G.) and that between the rear suspension and C.G. l_{ylf} and l_{ylr} are the distance between the left suspension and C.G. and that between the right suspension and C.G., respectively. z_{bi}, z_{wi} and w_i ($i = 1,2,3,4$) are the displacement of the sprung mass and unsprung mass, and in the i suspension, and the disturbance applied to the i tire.

3.2. The sliding mode controller

In order to simplify the control system of the full-car semi-active suspension with MR dampers, four independent sliding mode controllers are designed. Each controller is used to control one quarter of the car model shown in Fig. 6. In this way, the computational burden for the whole control system can be reduced. This is essential to obtaining a rapid response for various road conditions. Hence, a quarter-car model is considered to design these sliding mode controllers as shown in Fig. 7.

For the quarter-car model, the governing equations of motion can be expressed as follows:

$$M_{si}\ddot{z}_{bi} + f_{ksi} + f_{csi} = F_{MRi},\ M_{wi}\ddot{z}_{wi} - f_{ksi} - f_{csi} + f_{kti} = -F_{MRi} \tag{4}$$

where M_{si} is sprung mass.

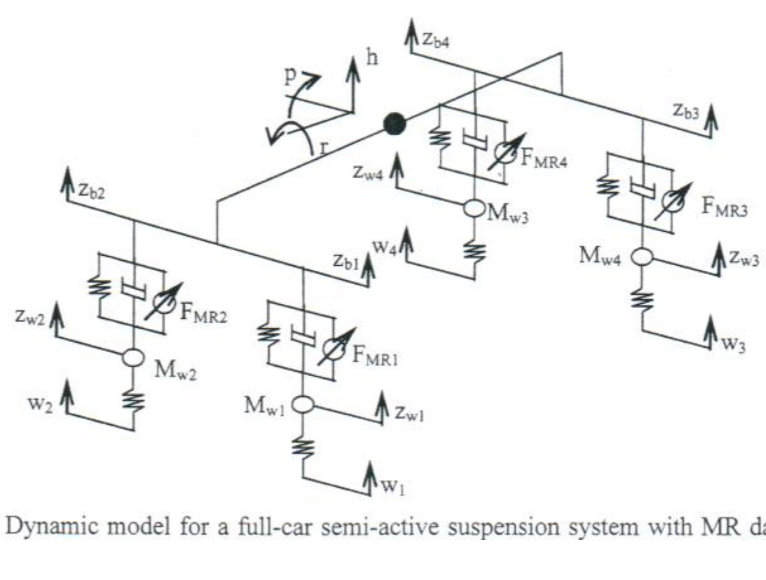

Fig. 6 Dynamic model for a full-car semi-active suspension system with MR dampers

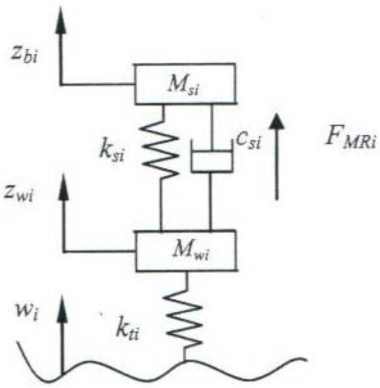

Fig. 7 A quarter-car model

The state vector is defined as

$$X_i = [X_{i1} \;\; X_{i2} \;\; X_{i3} \;\; X_{i4}]^T = [z_{bi}-z_{wi} \;\; \dot{z}_{bi} \;\; z_{wi}-w_i \;\; \dot{z}_{wi}]^T$$

So the state-space equation is obtained:

$$\dot{X}_i = A_i X_i + B_i F_{MRi} + E_i \dot{w}_i \tag{5}$$

where

$$A_i = \begin{bmatrix} 0 & 1 & 0 & -1 \\ -\dfrac{k_{si}}{M_{si}} & -\dfrac{c_{si}}{M_{si}} & 0 & \dfrac{c_{si}}{M_{si}} \\ 0 & 0 & 0 & 1 \\ \dfrac{k_{si}}{M_{wi}} & \dfrac{c_{si}}{M_{wi}} & -\dfrac{k_{ti}}{M_{wi}} & -\dfrac{c_{si}}{M_{wi}} \end{bmatrix}, B_i = \begin{bmatrix} 0 \\ \dfrac{1}{M_{si}} \\ 0 \\ -\dfrac{1}{M_{wi}} \end{bmatrix}, \text{ and } E_i = \begin{bmatrix} 0 \\ 0 \\ -1 \\ 0 \end{bmatrix}.$$

In fact, M_{si} may often vary due to the changing loading conditions. Here, we consider that M_{si} to be uncertain, it can be expressed as follows:

$$M_{si} = M_{si0} + \Delta M_{si} \quad |\Delta M_{si}| < 0.5 M_{si0} \tag{6}$$

where, M_{si0} is nominal sprung mass and ΔM_{si} is the uncertain part of sprung mass. This uncertainty can be written as:

$$\frac{1}{M_{si}} = \frac{1}{M_{si0} + \Delta M_{si}} = \frac{1}{M_{si0}}(1+\gamma) \quad |\gamma| < 1 \tag{7}$$

Substituting Eq. (7) into Eq. (5), the state-space equation can be expressed with the parameter uncertainty as follows:

$$\dot{X}_i = (A_{i0} + \Delta A_i)X_i + (B_{i0} + \Delta B_i)F_{MRi} + E_i \dot{w}_i \tag{8}$$

with A_{i0} and B_{i0} denoting the nominal parts, while ΔA_i and ΔB_i denoting the uncertain parts of the system matrixes A_i and B_i respectively.

The first step for designing a sliding mode controller is to determine a sliding mode surface:

$$S(X) = CX = 0 \tag{9}$$

where C is the surface gradient to be determined so that the sliding mode surface is asymptotically stable. A popular method to determine matrix C is to select a set of eigenvalues, eigenvector W associated with the desired eigenvalues can be expressed (El-Ghezawi, *et al.* 1983):

$$A_{i0}W - WJ = B_{i0}N \tag{10}$$

where J is Jordan-block form associated with desired eigenvalues and N is an arbitrary matrix chosen to provide linear combinations of the column B_{i0}.Thus, the surface gradient C can be defined by the inverse of $[W \vdots B_{i0}]$.

It is easy to determine the surface gradient matrix C using the above method. However, it will result in a particularly high control gain, in the other word, high energy supply is required to ensure system robustness. In order to solve the problem, in the present study, the sliding mode controller will be formulated based on an LQR control strategy. The total control force is divided into two parts. The first part is the linear part while the other part is the nonlinear part. The linear control force is determined by the LQR control and the nonlinear part is determined by the conventional sliding mode switching function as follows:

$$F_{MRi} = F_{MRlinear} + F_{MRnonlinear} \tag{11}$$

In order to determine a linear control force, LQR control for a quarter-car model is used. The cost function for LQR control can be expressed as follows:

$$J = \int_0^{\infty} (y_i^T Q_i y_i + rF_{MRi^2})dt \tag{12}$$

where, $y_i = [\ddot{z}_{bi} \;\; z_{bi} - z_{wi} \;\; z_{wi} - w_i]^T$ = the output which can be written as:

$$y_i = cX_i + dF_{MRi}. \tag{13}$$

Hence, the optimal gain matrix K is given by:

$$K = R^{-1}(B^T P + N^T) \tag{14}$$

Let $\quad Q = c^T Q_i c, N = c^T Q_i d, R = r + d^T Q_i d$

Then, P is the solution of the associated Riccati equation:

$$A^T P + PA - (PB + N)R^{-1}(B^T P + N^T) + Q = 0 \tag{15}$$

and the linear control force is obtained:

$$F_{MRlinear} = -KX = -R^{-1}(B^TP + N^T)X \tag{16}$$

For nonlinear part, first a sliding surface is defined:

$$S = CX = R^{-1}(B^TP + N^T)X \tag{17}$$

In this way, the nonlinear control force can be given by sliding mode control theory:

$$F_{MRnonlinear} = -F^*(CB)^{-1}sign(S) \tag{18}$$

Substituting Eq. (18), Eq. (16), and Eq. (11) into Eq. (5), the stability condition is identified as follows:

$$S\dot{S} = X^T(PB + N)R^{-1}R^{-1}(B^TP + N^T)(AX + BF_{MRi} + E\dot{w})$$

$$= X^T(PB + N)R^{-1}R^{-1}(B^TP + N^T)AX - R^{-1}(B^TP + N^T)BS^2 - F^*|S| + SR^{-1}(B^TP + N^T)E\dot{w}$$

$$= X^T[(PB + N)(B^TP + N^T)A + A^T(PB + N)(B^TP + N^T)]X/2R^2 - (B^TP + N^T)BS^2/R$$

$$-F^*|S| + SR^{-1}(B^TP + N^T)E\dot{w} \tag{19}$$

Since $(PB + N)(B^TP + N^T)$ is positive semi-definite, and A is stable, thus, the matrix $[(PB + N)(B^TP + N^T)A$ $+A^T(PB + N)(B^TP + N^T)]$ is negative semi-definite. Also, the scalar $(B^TP + N^T)BS^2/R$ is positive. Therefore, the first two terms in Eq. (19) is negative. In this case, the stability condition $S\dot{S} < 0$ can be satisfied when:

$$-F^*|S| + SR^{-1}(B^TP + N^T)E\dot{w} < 0 \tag{20}$$

We assume $|\dot{w}| \le \dot{w}_{\max}$, the above inequality is modified into:

$$F^* \ge |(B^TP + N^T)E/R|\dot{w}_{\max} \tag{21}$$

Since the nonlinear control force includes the sign function, undesirable chattering may occur. In order to reduce the chattering, a usual method is to replace the sign function by the saturation function with appropriated boundary layer thickness ε. However, boundary layer method has a tradeoff between chattering and robustness, it is impossible using boundary layer method to improve chattering and robustness at the same time. Fuzzy logic control (FLC) has been powerful in dealing with such systems as complex, ill-defined, nonlinear, or time-varying. FLC can be implemented by converting the linguistic control strategy of human experience or expert knowledge into an automatic control strategy. As it usually needs no mathematical model of the controlled system, it is relatively easy to implement and meet the requirement of real-time. The smooth control feature of FLC can be used to alleviate the chattering phenomenon of conventional SMC systems without sacrifice the robustness. This can be achieved by the merging of the FLC with the variable structure of the SMC to form a fuzzy sliding mode control (Hwang and Tomizuka 1994, Kurimoto, *et al.* 2000). In this hybrid control system, the advantage of the SMC lies in its applicability to modeling imprecision and external disturbances while the FLC provides smooth control action and reduces chattering.

4. The fuzzy-sliding mode controller

In this section, fuzzy logic control is introduced to design a fuzzy-sliding mode controller (FSMC). The rules of fuzzy-sliding mode controller can be described as follows (Kim and Lee 1995):

Rule1: If S is NB, then $F_{MRnonlinear}$ is PB
Rule2: If S is NM, then $F_{MRnonlinear}$ is PM
Rule3: If S is ZE, then $F_{MRnonlinear}$ is ZE
Rule4: If S is PM, then $F_{MRnonlinear}$ is NM
Rule5: If S is PB, then $F_{MRnonlinear}$ is NB

where *NB*, *NM*, *ZE*, *PM*, *PB* are linguistic terms of antecedent fuzzy set, they mean that negative big, negative medium, zero, positive medium, positive big. The manipulated variable $F_{MRnonlinear}$ is the output of the FSMC while the switching variable S is the input of the FSMC. In fact, the usually boundary layer method uses a linear interpolation of the control output between the positive and negative control value in the boundary layer while the FSMC uses nonlinear interpolation in the boundary layer. Fig. 8 shows the transfer characteristics of linear boundary layer and nonlinear FSMC.

Figs. 9 and 10 show the membership functions of S and $F_{MRnonlinear}$. The rules of the fuzzy sliding

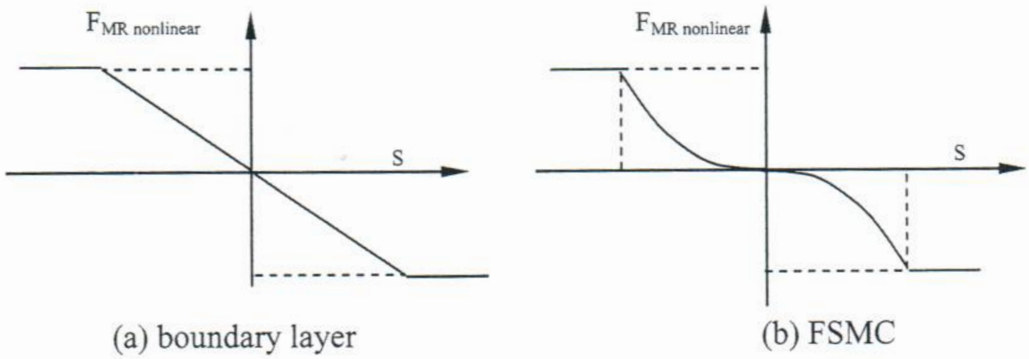

Fig. 8 transfer characteristics of boundary layer and FSMC

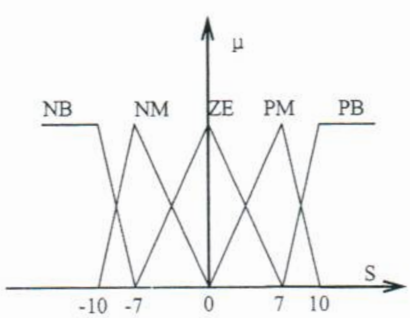

Fig. 9 The membership functions of S

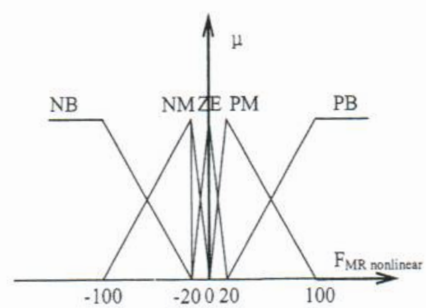

Fig. 10 The membership functions of $F_{MRnonlinear}$

mode controller have the general form of:

Rule i : If S is A_i, then $F_{MRnonlinear}$ is B_i, i=1,2,3,4,5

where A_i and B_i are labels of fuzzy sets representing the linguistic values of S and $F_{MRnonlinear}$ respectively, which are characterized by their membership functions. The output of the fuzzy-sliding mode controller is a fuzzy set of control. In order to obtain non-fuzzy value of control, a method of defuzzification called "center of gravity method" is used here:

$$F_{MRnonlinear} = \frac{\sum_{i=1}^{5} F_{MRnonlinear} \cdot \mu_{Bi}(F_{MRnonlinear})}{\sum_{i=1}^{5} \mu_{Bi}(F_{MRnonlinear})} \tag{22}$$

where $\mu_{Bi}(F_{MRnonlinear})$ is the corresponding membership function.

The control force F_{MRi} given by Eq. (10) is calculated in an active actuating manner. However, the MR damper is a semi-active actuator. Thus, the control damping force should be modified to meet semi-active constrained condition:

$$F_{MRi} = \begin{Bmatrix} F_{MRi} \; for \; F_{MRi}(\dot{z}_{bi} - \dot{z}_{wi}) > 0 \\ 0 \quad for \; F_{MRi}(\dot{z}_{bi} - \dot{z}_{wi}) \leq 0 \end{Bmatrix} \quad (i = 1,2,3,4) \tag{23}$$

5. Performance evaluation and discussions

The control characteristics for the full-car semi-active suspension system with MR dampers are evaluated under two types of road excitations. The first excitation is a single rectangular bump having the height of 0.01 *m* and the width of 0.5 *m*. It is used to reveal the transient response characteristics. In this bump excitation, the vehicle travels over the bump with a velocity of 3 *km/h*. The second type of road excitation is random road profiles which are used to evaluate the stable state response characteristics. As a typical random process, the power spectral density (PSD) of the road velocity excitation can be expressed as follows (Wang 2001):

$$G_{\dot{w}}(f) = (2\pi f)^2 G_w(f) = 4\pi^2 G_0 n_0^2 v \tag{24}$$

where n_0 is the reference spatial frequency $n_0 = 0.1(1/m)$. G_0 denotes the road roughness coefficient. In general, typical roads can been classified into eight classes according to different road roughness. In this paper, C type road ($G_0 = 256\times10^{-6} m^3$) is selected to evaluate the effectiveness of the proposed controller. Since the PSD of the velocity signal of the road roughness is independent of frequency, we can view it as a band-limited white-noise independent of frequency. The road disturbance can be obtained by integrating the white-noise signal produced by Eq. (24). The vehicle is assumed to travel at a constant speed of 20 *m/s* (72 *Km/hr*).

The system parameters of the full-car suspension with MR dampers are listed in Table 2.

Table 2 Parameters of the full-car model with MR dampers

Parameter	Unit	Value
M_s	kg	1583
I_{xx}/I_{yy}	kg m^2	531/2555
$M_{w1}/M_{w2}/M_{w3}/M_{w4}$	kg	48/48/74/74
$K_{s1}/K_{s2}/K_{s3}/K_{s4}$	N/m	35000/35000/34000/34000
$C_{s1}/C_{s2}/C_{s3}/C_{s4}$	Ns/m	600/600/600/600
$K_{t1}/K_{t2}/K_{t3}/K_{t4}$	N/m	220000/220000/220000/220000
I_{xf}/I_{xr}	m	1.116/1.438
$I_{ylf}/I_{yrf}/I_{ylr}/I_{yrr}$	m	0.77/0.77/0.765/0.765

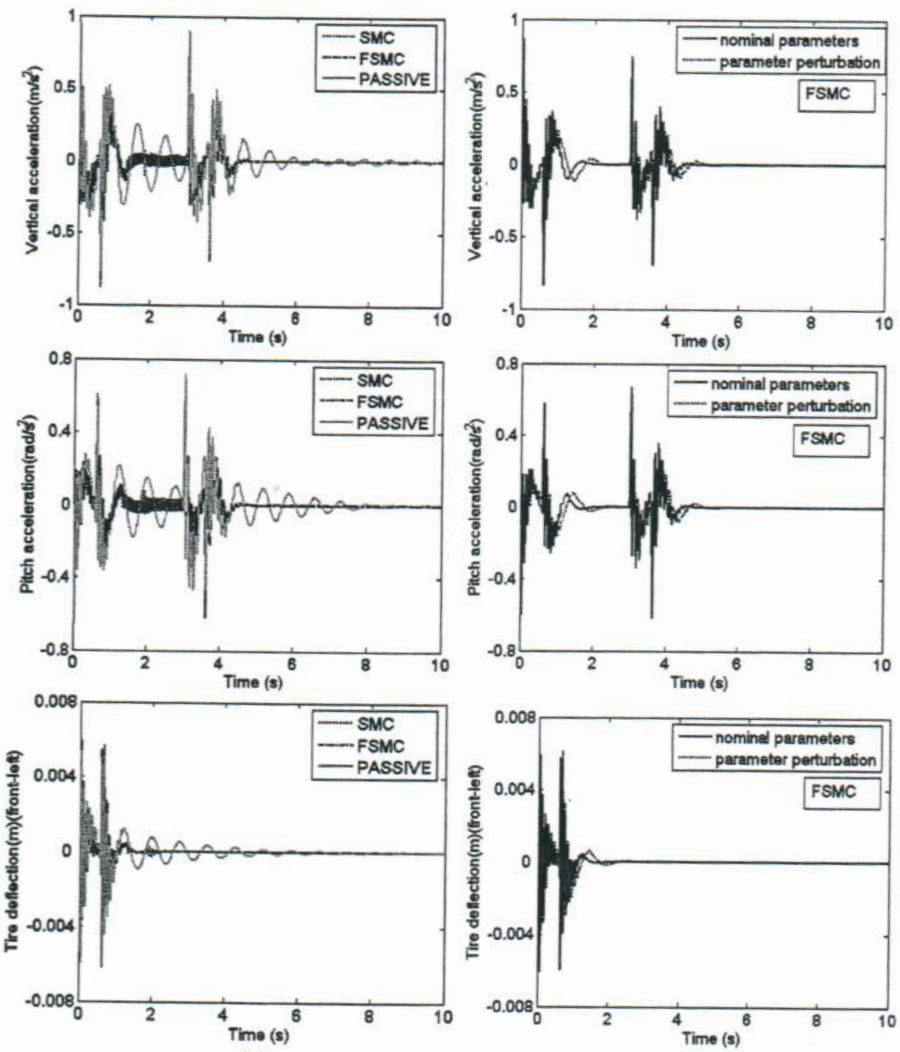

Fig. 11 Time responses of the full-car suspension with MR dampers for the bump excitation : (a) using different controller under nominal parameters and (b) comparison between nominal parameters and parameter perturbations in FSMC controller

The four independent LQR controllers are designed based on Eqs. (13-15) and (16). $Q_i = diag[q_{1i}, q_{2i}, q_{3i}]$ (i=1,2,3,4), q_{1i}, q_{2i} and q_{3i} represent the weighting factors which are selected to be $q_{1i} = 2.18\times10^4$, $q_{2i} = 9.9\times10^5$, $q_{3i} = 9.39\times10^6$ (i=1,2,3,4).

The optimal LQR gain matrices are obtained as follows:

$$K_1 = K_2 = [-1762.6 \;\; 725.7 \;\; 605.6 \;\; 21.3] \text{ and}$$
$$K_3 = K_4 = [-2716.8 \;\; 798.4 \;\; 967.8 \;\; 28].$$

For the SMC, $F_1^* = F_2^* = 121$, and $F_3^* = F_4^* = 192$.

For the FSMC, $S = \{-10 \; -7 \; 0 \; 7 \; 10\}$, and $F_{MRnonlinear} = \{-100 \;\; -20 \;\; 0 \;\; 20 \;\; 100\}$.

Fig. 11 presents the controlled time responses of the full-car semi-active suspension with MR dampers for the bump excitation. It can be observed that the vertical and pitch acceleration of sprung mass and tire deflection are substantially reduced by the sliding mode controller, the chattering of the SMC is smoothed by the proposed fuzzy-sliding mode controller (FSMC). The robust character of the proposed controller is studied by considering the parameter perturbations: $\Delta M = 791.5\ kg$, ΔI_{xx}=265.5 kg m^2, ΔI_{yy} = 1277.5 kg m^2. It can be seen that the FSMC displays good robustness in the presence of parameter perturbation.

Fig. 12 presents the controlled frequency response of the semi-active suspension with MR dampers when subjected to random excitation. It can be seen that the vertical acceleration, pitch acceleration, tire and suspension deflections are substantially reduced by FSMC controllers, especially at the resonant frequency of the vehicle body.

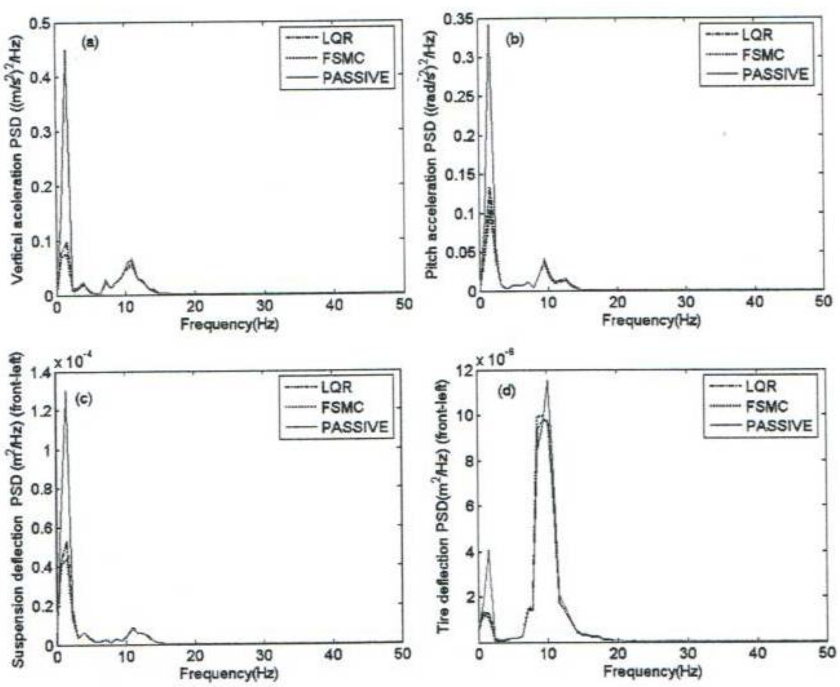

Fig. 12 Frequency responses of the full-car suspension with MR dampers for random excitation

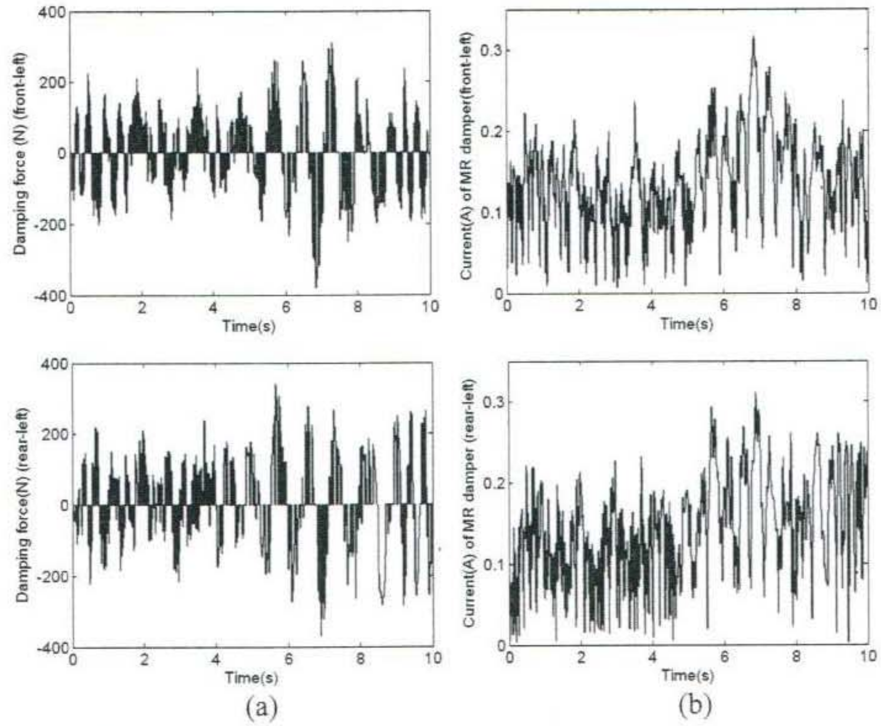

Fig. 13 The control damping force (a) and control current (b) for random excitation

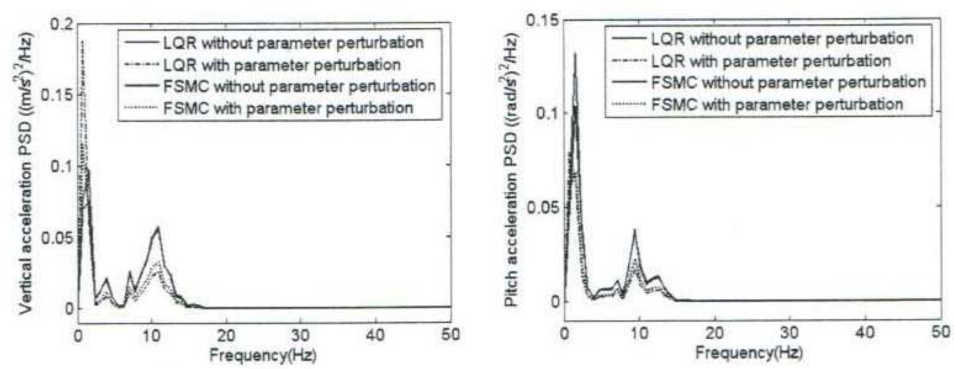

Fig. 14 The comparison of robust character using LQR and FSMC controller

Fig. 13 displays the control damping forces supplied by MR dampers and their control currents using the proposed FSMC controllers for the case of random excitation.

Fig. 14 demonstrates the robustness of FSMC controller. It can be seen that the robustness of nonlinear FSMC controller is much better than linear LQR controller. This is a very important feature due to vehicle dynamics change with road conditions. Table 3 is the comparison of cost functions using FSMC controller and LQR controller. The energy supply is required to increase 30% in order to provide a good robustness for FSMC controller. However, the total cost increases only 1%. This means that the design of FSMC controller is successful from energy consumption opinion.

Table 3 The comparison of cost functions using LQR and FSMC controllers

Controller	*Response cost*	*Energy cost*	*The total cost*
LQR	6.7633×10^6	1.517×10^6	8.2803×10^6
FSMC	6.3825×10^6	1.966×10^6	8.3485×10^6

6. Conclusions

An adaptive control system is developed for semi-active suspension systems of vehicles using magneto-rheological (MR) fluid dampers. MR dampers with the mix mode are designed and manufactured, and their field-dependent damping forces are experimentally evaluated. Four independent controllers are designed to suppress vehicle vibration. The siding mode controller based on LQR control is designed to reduce energy consumption. The smooth control feature of FLC is used to alleviate the chattering of conventional SMC systems by the merging of the FLC with the variable structure of the SMC to form a fuzzy sliding mode controller. A novel fuzzy sliding mode controller for semi-active suspensions with MR dampers is designed and fabricated. The bump and random excitation are used to evaluate the effectiveness of the proposed controller. The results show that the sliding mode controller based on LQR can substantially reduce the vertical, pitch and roll acceleration as well as tire deflection. When fuzzy control is merged into the sliding mode controller, the smooth feature of non-model based fuzzy control is demonstrated. Fuzzy control can be used to smooth the control response, improve the control quality. The control process using the proposed fuzzy sliding mode controller is stable and demonstrates a good robustness. The total cost function using fuzzy sliding mode controller is a litter bit higher than that using LQR controller. The control effectiveness and robustness are intensified by the novel fuzzy sliding mode controller compared with linear LQR controller.

Acknowledgements

This study was supported by a grant from the Chinese Nature Science Foundation (Grant No. 50475064).

References

Breese, D.G. and Gordaninejad, F. (2003), "Semi-active, fail-safe magneto-rheological fluid dampers for mountain bicycles", *Int. J. Vehicle Des.*, **33**(1/2/3), 128-138.

Choi, S.B., Choi, H.J., Lee, Y.S. and Han, M.S. (2003), "Vibration control of an ER seat suspension for a commercial vehicle", *J. Dyn. Syst.-T. ASME*, **125**, 60-68.

Choi, S.B., Lee, H.S. and Park, Y.P. (2002), "H ∞ Control performance of a full-vehicle suspension featuring magnetorheological dampers", *Vehicle Syst. Dyn.*, **38**(5), 341-360.

Choi, S.B., Choi, Y.T. and Park, D.W. (2000), "A sliding mode control of a full-car electrorheological suspension system via hardware in-the-loop simulation", *J. Dyn. Syst.-T. ASME*, **122**, 114-121.

Dyke, S.J., Spencer Jr, B.F., Sain, M.K. and Carson, J.D. (1996), "Modeling and control of magnetorheological dampers for seismic response reduction", *Smart Mater. Struct.*, **5**, 565-575.

El-Ghezawi, O.M., Zinober, A.S. and Billings, S.A. (1983), "Analysis and design of variable structure systems using a geometric approach", *Int. J. Control*, **38**, 657-671.

Ericksen, E.O. and Gordaninejad, F. (2003), "A magneto-rheological fluid shock absorber for an off-road motorcycle", *Int. J. Vehicle Des.*, **33**(1/2/3),139-152.

Gordaninejad, F. and Kelso, S.P. (2000), "Magneto-rheological fluid shock absorbers for HMMWV", *Proc. of SPIE Conf. on Smart Structures and Materials,* Newport Beach, CA, March.

Gordaninejad, F. and Kelso, S.P. (2000), "Fail-safe magneto-rheological fluid dampers for off- highway, high-payload vehicles", *J. Intel. Mater. Syst. Str.,* **11**(5), 395-406.

Hwang, Y.R. and Tomizuka, M. (1994), "Fuzzy smoothing algorithm for variable structure systems", *IEEE T. Fuzzy Syst.*, **2**, 277-284.

Inaudi, J.A. (1997), "Modulated homogeneous friction (MHF)", *Earthq. Eng. Struct. D.*, **26**, 361-376.

Kim, S.W. and Lee, J.J. (1995), "Design of a fuzzy controller with fuzzy sliding surface", *Fuzzy Sets Syst.*, **71**, 359-367.

Kurimoto, M., Yoshimura, T. and Hino, J. (2000), "An active suspension system of quarter-car models using sliding mode controller", *Transactions of the Japan Society of Mechanical Engineers (Series C)*, **66**, 468-475.

Leitmann, G. (1994), "Semi-active control for vibration attenuation", *J. Intel. Mater. Syst. Str.*, **5**, 841-846.

Liu, Y., Gordaninejad, F., Evrensel, C.A., Dogruer, U., Yeo, M.S., Karakas, E.S. and Fuchs, A. (2003), "Temperature dependent skyhook control of HMMWV suspension using a fail-safe magneto-rheological damper", *Proc. SPIE Smart Structures and Materials Conf., Industrial and Commercial Applications*, Ed. by E.H. Anderson, March, **5054**, 332-340.

Liu, Y., Gordaninejad, F., Evrensel, C.A. and Hitchcock, G. (2001), "An experimental study on fuzzy logic vibration control of a bridge using fail-safe magneto-rheological fluid dampers", *Smart Systems for Bridges, Structures, and Highways, Proc. of SPIE Conference on Smart Materials and Structures*, Ed. by Chi Liu, **4330**, 281-288.

LORD Materials Business Unit (1999), "Designing with MR fluids", *Engineering Note*.

McClamroch, N.H. and Gavin, H.P. (1995), "Closed loop structural control using electrorheological dampers", *Proc. of the American Control Conf.,* Washington D.C.

Man, P.D., Mistrot, P., Verschueren, J.P. and Preumont, A. (2005), "An investigation of a semi-active suspension for a fork lift truck", *Vehicle Syst. Dyn.,* **43**(2), 107-119.

Patten, W.N., Kuo, C.C., He, Q., Liu, L. and Sack, R.L. (1994a), "Seismic structural control via hydraulic semiactive vibration dampers (SAVD)", *Proc. of the First World Conf. on Struct. Control*, International Association for Structural Control, Los Angeles, CA.

Patten, W.N., Kuo, C.C., He, Q., Liu, L. and Sack, R.L. (1994b), "Suppression of vehicle-induced bridge vibration via hydraulic semiactive vibration dampers", *Proc. of the First World Conf. on Structural Control,* Pasadena, CA.

Sean, P.K. (2001), "Experimental characterization of commercially practical magnetorheological fluid damper technology", *SPIE Conf. on Smart Structure and Materials*, San Diego, CA, March.

Song, X.B. and Ahmdian, M. (2004), "Study of semiactive adaptive control algorithms with magneto-rheological seat suspension", *SAE paper,* 2004-01-1648.

Slotine, J.J. and Sastry, S.S. (1983), "Tracking control of nonlinear systems using sliding surfaces, with application to robot manipulators", *Int. J. Control*, **38**, 465-492.

Sun, L. and Goto, Y. (1994), "Application of fuzzy theory to variable dampers for bridge vibration control", *Proc. First World Conf. Structural Control*, Pasadena, CA.

Wang, E.R., Ma, X.Q., Rakheja, R. and Su, C.Y. (2003), "Semi-active control of vehicle vibration with MR-dampers", *Proc. of the 42th IEEE Conf. on Decision and Control* , Hawaii , USA, December.

Wang, J.Y. (2001), *Theory of Ground Vehicles*, 3rd ed. New York: John Wiley.

Yao, G.Z., Yap, F.F., Chen, G., Li, W.H. and Yao, S.H. (2002), "MR damper and its application for semi-active control of vehicle suspension system", *Mechatronics,* **12**, 963-973.

Yang, G., Spencer, B.F., Carlson, J.D. and Sain, M.K. (2002), "Large-scale MR fluid dampers: modeling and dynamic performance considerations", *Eng. Struct.,* **24**, 309-323.

Yokoyama, M., Hedrick, J.H. and Toyama, S. (2001), "A model following sliding mode controller for semi-active suspension systems with MR dampers", *Proc. of the American Control Conf.*, Arlington, VA, June.